PHILOSOPHICAL TRANSACTIONS A

rsta.royalsocietypublishing.org

Research

Cite this article: He Z, Qian Q, Zhang Z, Meng Q, Zhou H, Jiang Z, Han B. 2015 Synthesis of higher alcohols from CO_2 hydrogenation over a PtRu/Fe_2O_3 catalyst under supercritical condition. *Phil. Trans. R. Soc. A* **373**: 20150006. http://dx.doi.org/10.1098/rsta.2015.0006

Accepted: 7 July 2015

One contribution of 12 to a discussion meeting issue 'Supercritical fluids: green solvents for green chemistry?'

Subject Areas:
green chemistry, physical chemistry

Keywords:
CO_2 hydrogenation, higher alcohols, bimetallic catalysis

Author for correspondence:
Buxing Han
e-mail: hanbx@iccas.ac.cn

Downloaded from https://royalsocietypublishing.org/ on 04 March 2022

Synthesis of higher alcohols from CO_2 hydrogenation over a PtRu/Fe_2O_3 catalyst under supercritical condition

Zhenhong He, Qingli Qian, Zhaofu Zhang, Qinglei Meng, Huacong Zhou, Zhiwei Jiang and Buxing Han†

Beijing National Laboratory for Molecular Sciences, CAS Key Laboratory of Colloid, Interface and Chemical Thermodynamics, Institute of Chemistry, Chinese Academy of Sciences, Beijing 100190, People's Republic of China

Hydrogenation of CO_2 to alcohols is of great importance, especially when producing higher alcohols. In this work, we synthesized heterogeneous PtRu/Fe_2O_3, in which the Pt and Ru bimetallic catalysts were supported on Fe_2O_3. The catalyst was used to catalyse CO_2 hydrogenation to alcohols. It was demonstrated that the activity and selectivity could be tuned by the bimetallic composition, and the catalyst with a Pt to Ru molar ratio of 1 : 2 (Pt_1Ru_2/Fe_2O_3) had high activity and selectivity at 200°C, which is very low for heterogeneous hydrogenation of CO_2 to produce higher alcohols. The conversion and the selectivity increased with increasing pressures of CO_2 and/or H_2. The catalyst could be reused at least five times without any obvious change in activity or selectivity.

1. Introduction

The rapid increase in the CO_2 concentration in the atmosphere is the cause of the greenhouse effect, which is the main reason for global warming [1]. From a synthetic chemistry point of view, CO_2 is an abundant, non-toxic, non-flammable and renewable carbon resource. Transformation of CO_2 to valuable chemicals, such as alcohols and hydrocarbons, is very interesting [2]. However, CO_2 is the fully oxidized carbon and is very stable. In this respect, development of a highly active catalyst is crucial for CO_2 transformation.

†Present address: Institute of Chemistry, Chinese Academy of Sciences, Zhongguancun North First Street 2, Beijing 100190, People's Republic of China.

THE ROYAL SOCIETY PUBLISHING

© 2015 The Author(s) Published by the Royal Society. All rights reserved.

Downloaded from https://royalsocietypublishing.org/ on 04 March 2022

CO_2 hydrogenation has been investigated extensively, and many heterogeneous and homogeneous catalysts have been developed for the synthesis of methanol [3–5]. Hydrogenation of CO_2 to ethanol is interesting because ethanol has some expected properties, such as it is non-toxic and easy to store and transport, and it has a higher energy density than methanol [6]. In addition, the higher alcohols are hydrogen carriers and fuels, precursors for important platform chemicals such as olefins, and reagents in the preparation of plasticizers and detergents [7]. Different catalysts have been used for producing higher alcohols, such as the Rh-based catalysts [8–11], CoMoS catalyst [12], K/Cu–Zn–Fe catalyst [13], the physically mixed Fe-based and Cu-based catalysts [14] and the homogeneous Ru–Co catalyst [15]. However, generation of higher alcohols from CO_2 hydrogenation is still challenging [16]. Relatively few works have focused on this topic, and, generally speaking, the reaction efficiency is low or a high temperature is required. The development of effective catalysts under mild conditions is highly desirable.

The advantages of bimetallic catalysis have long been recognized. The hybrid sites created from the synergistic combination of two metals results in high catalytic efficiency. For example, the Al_2O_3-supported Fe–Co bimetallic catalyst exhibited a high activity for the synthesis of olefin-rich C_{2+} hydrocarbons from CO_2 hydrogenation. The combination of a small amount of Co with Fe led to a dramatic bimetallic promotion of C_{2+} hydrocarbon synthesis [17]. Pt–Cu bimetallic catalysts exhibited a strong synergistic effect in catalysing methanol synthesis from CO_2 hydrogenation [18]. The Ru–Pt core–shell nanoparticle was also found to be more active than monometallic nanoparticle catalysts in catalysing the oxidation of CO [19], and so on. In this work, we prepared an Fe_2O_3-supported Pt–Ru bimetallic catalyst for synthesizing higher alcohols from CO_2 hydrogenation. It was found that the Pt_1Ru_2/Fe_2O_3 catalyst exhibited a high activity and high selectivity towards higher alcohols under relatively low temperature, and the pressure of the CO_2 and/or H_2 affected the reaction efficiency significantly.

2. Experimental section

(a) Materials

$Fe(NO_3)_3 \cdot 9H_2O$ (greater than 98.5%), $H_2PtCl_6 \cdot 6H_2O$ (99.9%) and $RuCl_3 \cdot 3H_2O$ (99.9%) were obtained from J&K Chemicals. The solvent, 1,3-dimethyl-2-imidazolidinone (DMI, 99%), was purchased from TCI Shanghai Co, Ltd. CO_2 (99.99%), H_2 (99.99%) and N_2 (99.95%) were provided by Beijing Analytical Instrument Company.

(b) Preparation and characterization of the $PtRu/Fe_2O_3$ catalyst

The $PtRu/Fe_2O_3$ catalysts were prepared by a facile co-precipitation method. In a typical synthesis, $H_2PtCl_6 \cdot 6H_2O$ (16 mg), $RuCl_3 \cdot 3H_2O$ (38 mg) and $Fe(NO_3)_3 \cdot 9H_2O$ (2.62 g) were dissolved in 30 ml degassed water, and then the mixture was added dropwise to 80 ml Na_2CO_3 solution (0.5 mol l^{-1}) over 1 h. After the mixture was stirred for another 1 h, the precipitate was separated by centrifugation and washed with distilled water (300 ml), and then dried at 100°C for 12 h. The solid was subjected to calcination at 400°C for 5 h, and then reduced at 400°C for 1 h under hydrogen flow; it was subsequently passivated with 1% oxygen in N_2 at room temperature for 30 min. In the end, the $PtRu/Fe_2O_3$ catalyst with a Pt to Ru molar ratio of 1 : 2 (1.48 wt% Pt and 2.96 wt% Ru) was obtained (denoted as Pt_1Ru_2/Fe_2O_3). For comparison, other catalysts such as Pt/Fe_2O_3, Ru/Fe_2O_3, Pt_1Ru_1/Fe_2O_3 (Pt to Ru molar ratio of 1 : 1), Pt_2Ru/Fe_2O_3 (Pt to Ru molar ratio of 2 : 1) and $PtRu_3/Fe_2O_3$ (Pt to Ru molar ratio of 1 : 3) were also prepared using the same procedure.

The as-prepared catalyst was characterized by X-ray diffraction (XRD), X-ray photoelectron spectroscopy (XPS), transmission electron microscopy (TEM) and temperature-programmed reduction by H_2 (H_2-TPR). The actual Pt and Ru loadings in the catalyst were detected by inductively coupled plasma atomic emission spectroscopy (ICP-AES, VISTA-MPX). The XRD was recorded on a Rigaku D/max 2500 with nickel-filtered Cu-Kα ($\lambda = 0.154$ nm) radiation operated

Downloaded from https://royalsocietypublishing.org/ on 04 March 2022

at 40 kV and 20 mA. A continuous mode was used for collecting data in the 2θ range from 15° to 80° at a scanning speed of 5° min^{-1}. The surface composition and the binding energy (B.E.) of the catalysts were determined by XPS on an ESCALab 220I-XL electron spectrometer from VG Scientific using 300 W Al-Kα radiation with a hemispherical energy analyser. The binding energies were calibrated with the C_1s level of adventitious carbon at 284.5 eV as the internal standard reference. The TEM images of the catalysts were obtained using a JEOL-2011 electron microscope operated at 120 kV. The reduction behaviours were studied by H_2-TPR performed in a conventional atmospheric quartz flow reactor (3 mm i.d.) (AutoChem II 2950 HP Chemisorption Analyzer; Micromeritics). Before the tests, the catalysts were heated at 300°C for 30 min under Ar at a flow rate of 50 ml min^{-1}. Then the temperature was reduced to 50°C and a 10% H_2–Ar mixture was flowed through the catalyst at a rate of 30 ml min^{-1}. The temperature was linearly raised from 50 to 800°C at a heating rate of 10°C min^{-1}. The effluent gas was analysed using a thermal conductivity detector (TCD).

(c) CO_2 hydrogenation and hot filtration test

The CO_2 hydrogenation was carried out in a 16 ml Teflon-lined stainless steel reactor in batch operation mode. In a typical experiment, the catalyst (20 mg) and the solvent (DMI; 1.0 ml) were loaded in the reactor. The reactor was flushed three times with CO_2, and then it was heated to 200°C. Subsequently, H_2 and CO_2 were charged and the reaction was performed for the desired time. Upon completion of the reaction, the reactor was cooled in ice-water, and then the gas was collected and analysed by HP 4890 GC with a TCD (Carbosieve B column; the GC oven was heated from 80°C to 200°C at a rate of 10°C min^{-1} and held at 200°C for 12 min). The liquid products were analysed in a HP 7890B GC with a flame ionization detector (HP-5 column with an optimized temperature programme at a rate of 40°C min^{-1} from 40°C to 270, and then held at 270°C for 10 min) using toluene as an internal standard. The selectivity of alcohols and hydrocarbons was calculated on the basis of the amount of carbon. In the recycling experiment, the solid catalyst was separated by centrifugation and washed with ether (3 × 3 ml), dried and then used for the next run. The hot filtration test was carried out under typical reaction conditions. After 5 h, the catalyst was filtered, and the resulting filtrate was placed under the same conditions as the original reaction and also followed by GC.

3. Results and discussion

(a) Characterization of the $PtRu/Fe_2O_3$ catalyst

Figure 1 shows the XRD patterns of Fe_2O_3, unreduced Pt_1Ru_2/Fe_2O_3 and the fresh (reduced) Pt_1Ru_2/Fe_2O_3 catalyst. Both the support and unreduced catalysts displayed peaks at $2\theta = 24.1$, 33.2, 35.6, 40.9, 49.5, 54.1, 57.5, 62.4 and 64.0, corresponding to (012), (104), (110), (113), (024), (116), (018), (214) and (300) of Fe_2O_3 (JCPDS PDF 33–0664), respectively (figure 1*a*,*b*). After reduction, the Fe_2O_3 patterns disappeared, but some new peaks appeared at 30.1, 35.5, 37.1, 43.1, 53.5, 62.6 and 44.7, 65.0, which were assigned to Fe_3O_4 (JCPDS PDF 65–3107) ((220), (311), (222), (400), (422), (440)) and Fe (JCPDS PDF 06–0696) ((110) and (200)), respectively. The results demonstrated that, after reduction, the Fe_2O_3 support was reduced partly to Fe_3O_4 and Fe(0). No Pt, Ru or Pt_1Ru_2 nanoparticles were found due to low loading or poor crystallization.

The chemical valence and surface composition of the unreduced catalyst and the fresh catalyst were detected by XPS, and the results are given in figure 2. It can be seen from figure 2*a*–*c* that, in the unreduced catalyst, the Pt and Ru species on the Pt_1Ru_2/Fe_2O_3 catalyst were mainly Pt^{2+}, Pt^{4+} and Ru^{3+}, respectively. The Pt XPS line exhibited Pt^{2+} $4f_{7/2}$ and $4f_{5/2}$ core level peaks at 73.1 and 78.4 eV, and Pt^{4+} $4f_{7/2}$ and $4f_{5/2}$ core level peaks at 74.5 and 81.3 eV, respectively. The Ru XPS line showed Ru^{2+} $3p_{3/2}$ and Ru^{4+} $3p_{3/2}$ species at 463.7 eV and 467.0 eV, respectively. The Fe species was Fe_2O_3, and Fe^{3+} $2p_{3/2}$ and Fe^{3+} $2p_{1/2}$ appeared at 710.6 eV and 724.2 eV, respectively (Fe_2O_3). In the spectra in figure 2*d*, the Pt XPS line of the fresh catalyst, two new peaks appeared at

Downloaded from https://royalsocietypublishing.org/ on 04 March 2022

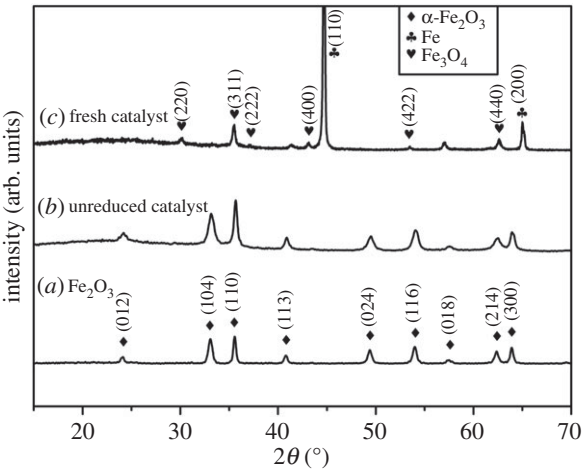

Figure 1. XRD patterns of (*a*) Fe_2O_3, (*b*) unreduced Pt_1Ru_2/Fe_2O_3 catalyst and (*c*) the fresh Pt_1Ru_2/Fe_2O_3 catalyst (reduced).

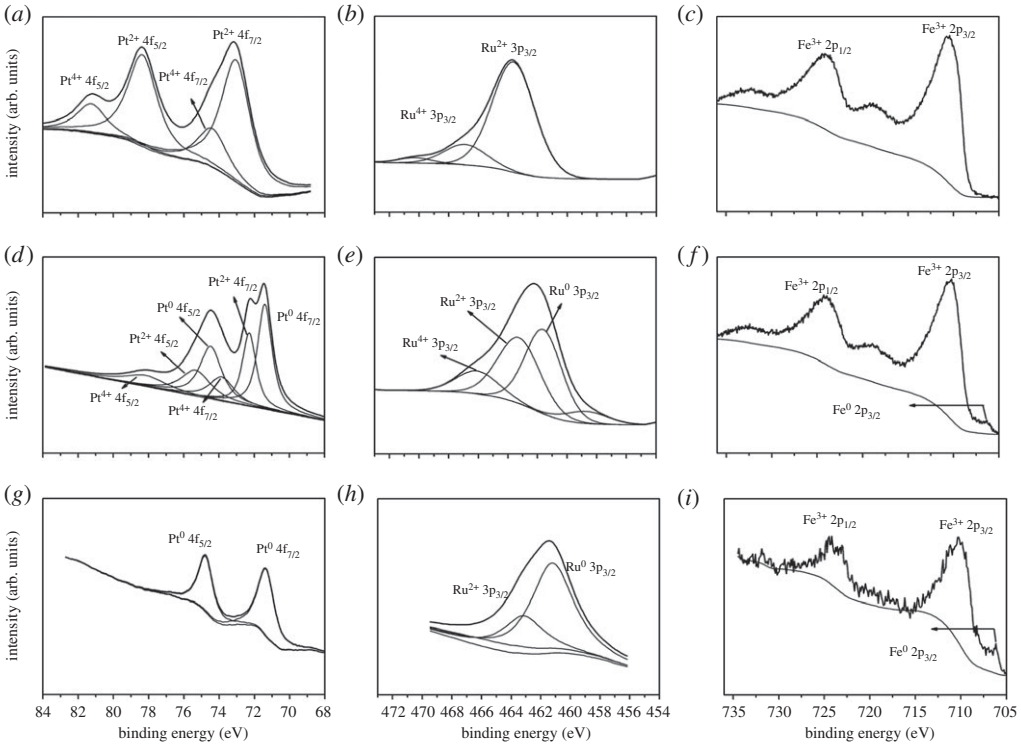

Figure 2. XPS of the unreduced Pt_1Ru_2/Fe_2O_3 (*a*, Pt; *b*, Ru; *c*, Fe), the fresh Pt_1Ru_2/Fe_2O_3 catalyst (*d*, Pt; *e*, Ru; *f* Fe) and the catalyst after three uses (*g*, Pt; *h*, Ru; *i*, Fe).

71.4 eV and 74.5 eV, which were attributed to the Pt^0 $4f_{7/2}$ and $4f_{5/2}$, respectively [20]. Meanwhile, in the Ru XPS line, the peak that appeared at 461.7 eV was Ru^0 $3p_{3/2}$ (figure 2*e*) [21]. The peak located at 706.8 eV was Fe^0 $2p_{3/2}$ [22]. The results indicated that, after the reduction, the Pt and Ru species were reduced to Pt^0 and Ru^0, and the Fe_2O_3 was partly reduced to Fe^0. The oxidized Pt and Ru were mainly due to surface oxygen passivation. The results agreed qualitatively with

Downloaded from https://royalsocietypublishing.org/ on 04 March 2022

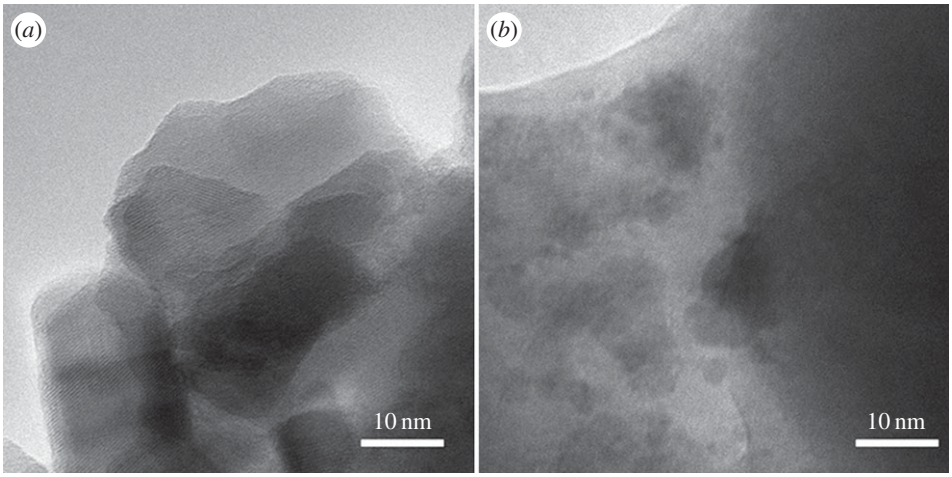

Figure 3. TEM images of the (*a*) unreduced and the (*b*) fresh Pt_1Ru_2/Fe_2O_3 catalyst (reduced).

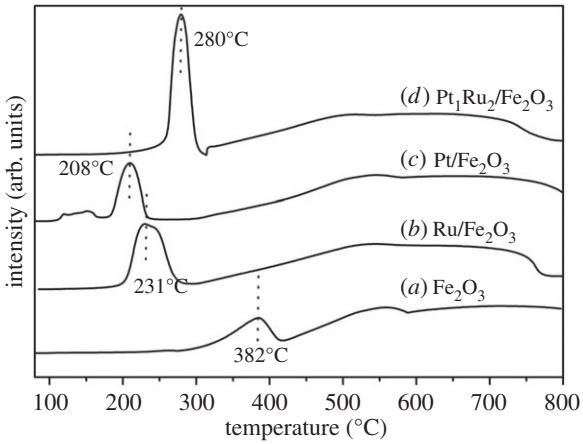

Figure 4. TPR profiles of (*a*) Fe_2O_3, (*b*) Ru/Fe_2O_3, (*c*) Pt/Fe_2O_3 and (*d*) Pt_1Ru_2/Fe_2O_3.

those of the XRD study. The Pt_1Ru_2/Fe_2O_3 catalyst that was used three times was also detected by XPS (figure 2*g*–*i*). It was found in the used catalyst, and the Pt and Ru were still immobilized on the Fe_2O_3 support although they were mostly reduced to Pt^0 and Ru^0.

The unreduced Pt_1Ru_2/Fe_2O_3 and the fresh catalysts were characterized by TEM. In the unreduced catalyst, there were no Pt and Ru nanoparticles. After the reduction, the Pt and Ru species were reduced to metal nanoparticles with size of 2–5 nm (figure 3).

To test the reduction behaviour of Fe_2O_3-supported Pt and Ru, temperature-programmed reduction of H_2 tests were carried out, and the results are shown in figure 4. For comparison, the Fe_2O_3 support was also prepared and tested. In the curve of figure 4*a*, two peaks appeared at 382°C and 550°C. The first reduction peak at 382°C was related to the reduction of Fe_2O_3 to Fe_3O_4. The high-temperature reduction peak at 550°C was attributed to the reduction of Fe_3O_4 to the FeO species [23,24]. However, using the supported catalysts, such as Ru/Fe_2O_3, Pt/Fe_2O_3 and Pt_1Ru_2/Fe_2O_3, the reduction temperatures of the Fe_2O_3 to Fe_3O_4 were 231°C, 208°C and 280°C, respectively, which were all lower than that of the pure Fe_2O_3 (figure 4*b*–*d*). The results showed that Pt, Ru and Pt–Ru could catalyse the reduction of Fe_2O_3, owing to the interaction between Ru, Pt, Pt–Ru and Fe_2O_3. Combined with the results of XPS and XRD, it can be deduced that, with

Downloaded from https://royalsocietypublishing.org/ on 04 March 2022

Table 1. Catalytic performances of CO_2 hydrogenation. Reaction conditions: P_{H2} 8 MPa, P_{CO2} 12 MPa, catalyst 20 mg, reaction time 15 h, DMI 1.0 ml.

entry	catalyst	T (°C)	selectivity (C%)					activity ($mmol_{CO_2}\ g_{cat}^{-1}\ h^{-1}$)
			C_1OH	$C_{2+}OH$	C_{1-4}^{a}	C_{5+}^{a}	CO	
1	Fe_2O_3	200	0	0	85.3	14.7	0	0.1
2	Pt/Fe_2O_3	200	8.9	0.1	71.6	19.4	0	2.5
3	Ru/Fe_2O_3	200	5.9	0.3	84.1	9.7	0	2.1
4	Pt_1Ru_3/Fe_2O_3	200	6.1	11.5	75.9	6.4	0.1	1.9
5	Pt_1Ru_2/Fe_2O_3	200	6.3	36.0	50.5	6.8	0.4	2.4
6	Pt_1Ru_1/Fe_2O_3	200	14.5	16.8	59.5	8.9	0.3	1.9
7	Pt_2Ru_1/Fe_2O_3	200	18.9	11.8	52.3	16.7	0.3	2.6
8	Pt_1Ru_2/Fe_2O_3	160	23.6	12.6	54.1	9.1	0.6	1.2
9	Pt_1Ru_2/Fe_2O_3	180	15.6	22.9	50.6	10.4	0.5	1.9
10	Pt_1Ru_2/Fe_2O_3	220	5.9	28.4	52.5	12.7	0.5	3.2

[a] C_{1-4} and C_{5+} stand for hydrocarbons with carbon numbers of 1–4 and higher than 5, respectively.

the Pt_1Ru_2/Fe_2O_3 catalyst, the Fe_2O_3 support was partly reduced to Fe_3O_4. Meanwhile, Fe(0) was formed after reduction under H_2 at 400°C, which was similar to the previous report [25].

(b) Catalytic performances of CO_2 hydrogenation to higher alcohols

As mentioned above, generally, the products of CO_2 hydrogenation contain alcohols and hydrocarbons. Tuning the selectivity of alcohols and hydrocarbons is very interesting in CO_2 hydrogenation. At first, the Fe_2O_3- and Fe_2O_3-supported catalysts were screened to synthesize higher alcohols from CO_2 hydrogenation. The hydrocarbons, especially the C_{1-4} hydrocarbons, could be generated over Fe_2O_3 under the given conditions, although the activity was only 0.1 $mmol_{CO_2}\ g_{cat}^{-1}\ h^{-1}$ (table 1, entry 1), indicating that CO_2 could be over-hydrogenated to hydrocarbons under catalysis with Fe_2O_3. The supported catalysts, such as Ru/Fe_2O_3, Pt/Fe_2O_3 and Pt_1Ru_2/Fe_2O_3, were used in the CO_2 hydrogenation. The C_{2+} alcohols could be obtained with the Pt/Fe_2O_3 and Ru/Fe_2O_3 catalysts, but the selectivity was much lower than that of methanol. For example, the Pt/Fe_2O_3 catalyst yielded 8.9% selectivity for methanol and 0.1% for C_{2+} alcohols; the Ru/Fe_2O_3 yielded 5.9% selectivity for methanol and 0.3% for C_{2+} alcohols (table 1, entries 2 and 3). On the contrary, the bimetallic catalyst Rh_1Ru_2/Fe_2O_3 favoured the generation of C_{2+} alcohols with a selectivity of 36.0%, which was much higher than that for methanol (6.3%; table 2, entry 5). As mentioned above, the Fe_2O_3-supported bimetallic catalyst showed excellent catalytic performance compared with the Fe_2O_3-supported monometallic catalyst. However, this enhancement of the catalytic performance was highly dependent on the composition the bimetallic catalysts, similar to those reported in the literature for other reactions [26,27]. For example, the selectivities for methanol and higher alcohols were, respectively, 14.5% and 16.8% with the Pt_1Ru_1/Fe_2O_3 catalyst (table 1, entry 6). The Pt_2Ru_1/Fe_2O_3 catalyst showed 18.9% and 11.8% selectivity for methanol and higher alcohols, respectively (table 1, entry 7).

The effect of temperature on CO_2 hydrogenation when using the Pt_1Ru_2/Fe_2O_3 catalyst was investigated in the temperature range of 160°C to 200°C (table 1, entries 8, 9, 5 and 10). It can be seen from the table 1 that a lower temperature (160°C) favoured the formation of methanol (23.6% methanol versus 12.6% C_{2+} alcohols) (table 1, entry 8). The content of higher alcohols increased with increasing temperature. In this respect, a high temperature was beneficial for the formation

Downloaded from https://royalsocietypublishing.org/ on 04 March 2022

Table 2. Effect of the H_2 and CO_2 pressure on the catalytic performances in CO_2 hydrogenation over Pt_1Ru_2/Fe_2O_3. Reaction conditions: catalyst 20 mg, reaction time 15 h, DMI 1.0 ml.

			selectivity (C%)					
entry	P_{H_2}	P_{CO_2}	C_1OH	$C_{2+}OH$	C^a_{1-4}	C^a_{5+}	CO	activity ($mmol_{CO_2}\ g_{cat}^{-1}\ h^{-1}$)
1	4	4	3.1	3.7	68.7	24.5	0	0.5
2	4	6	3.5	3.9	67.9	24.7	0	0.8
3	4	8	4.2	12.7	64.3	18.7	0.1	1.3
4	4	12	5.9	22.5	53.1	18.2	0.3	1.5
5	4	16	6.4	25.8	53.4	13.9	0.5	1.6
6	8	4	5.2	4.4	69.1	21.0	0.3	0.9
7	8	6	5.8	8.9	62.2	22.7	0.4	1.2
8	8	8	5.9	16.5	53.6	23.5	0.5	1.9
9	8	10	6.2	25.9	51.5	15.9	0.5	2.4
10	8	12	6.3	36.0	50.5	6.8	0.4	2.4

[a] C_{1-4} and C_{5+} stand for hydrocarbons with carbon numbers of 1–4 and higher than 5, respectively.

of higher alcohols. At the same time, the selectivity for hydrocarbons also became higher (table 1, entries 8–10).

The effect of CO_2 pressure on the reaction was studied and the results are summarized in table 2. Increasing the pressure of CO_2 could improve both the catalytic activity and the selectivity for higher alcohols. For example, at a fixed H_2 pressure of 4 MPa, the catalytic activities were 0.5, 1.3 and 1.6 $mmol_{CO2}\ g_{cat}^{-1}\ h^{-1}$, and the $C_{2+}OH$ selectivities were 3.7%, 12.7% and 25.8% (compared with the methanol selectivities of 3.1%, 4.2% and 6.4%, respectively) under a CO_2 pressure of 4, 8 and 16 MPa, respectively (table 2, entries 1, 3 and 5). A similar tendency was observed when the H_2 pressure was 8 MPa (table 2, entries 6–10). For example, the activities changed from 0.9 to 2.4 $mmol_{CO2}\ g_{cat}^{-1}\ h^{-1}$ and the $C_{2+}OH$ selectivities increased from 4.4% to 36.0%, respectively (table 2, entries 6 and 10), as the CO_2 pressure increased from 4 to 12 MPa. The results demonstrated that the higher CO_2 pressure could give a higher catalytic activity and $C_{2+}OH$ selectivity. In general, the rate of hydrogenation is usually slow due to the low solubility of hydrogen in common organic solvents [28]. High-pressure CO_2 can expand the organic solvents [29], which can enhance the dissolution of the H_2 and improve the efficiency of the reactions [30]. In our work, an increase in CO_2 pressure could increase the concentrations of H_2 and CO_2, which may be one of the main reasons for the enhanced catalytic activity and selectivity for C_{2+} alcohols. The results in table 2 also demonstrate that the higher H_2 pressure enhanced the reactivity mainly due to the fact that the solubility of H_2 in the liquid is higher at a higher H_2 pressure.

(c) Reusability of the catalyst and hot filtration test

The reusability of the Pt_1Ru_2/Fe_2O_3 catalyst was tested. In this experiment, the catalyst was separated from the reaction mixture by a centrifugation method after the reaction, and was used for the next run after it had been washed and dried. The results are shown in figure 5. It was demonstrated that the catalyst could be re-used at least five times without any obvious change in activity and selectivity. The ICP results showed that the Pt and Ru leaching was 0.8 ppm and 1.3 ppm, respectively, after the reaction. Furthermore, in the hot filtration test, no additional CO_2 was consumed after the catalyst was filtrated off (figure 6). These results and the XPS characterization (figure 2) clearly indicated that the Pt_1Ru_2/Fe_2O_3 catalyst possessed good stability in the catalytic reaction.

Downloaded from https://royalsocietypublishing.org/ on 04 March 2022

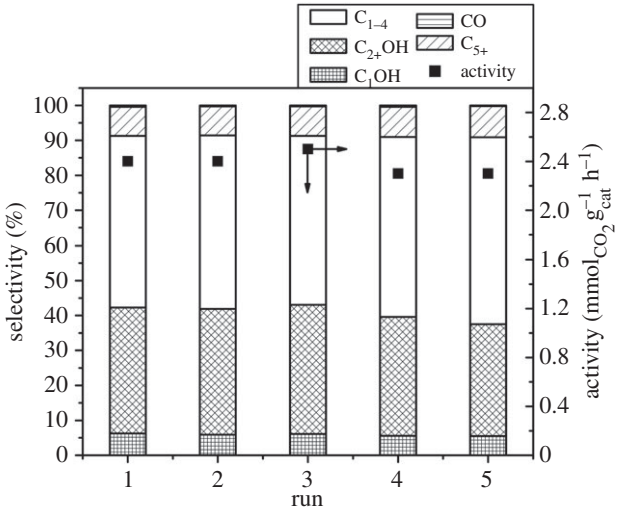

Figure 5. The reusability of the Pt_1Ru_2/Fe_2O_3 catalyst in CO_2 hydrogenation. Reaction conditions were the same as those of entry 10 in table 2.

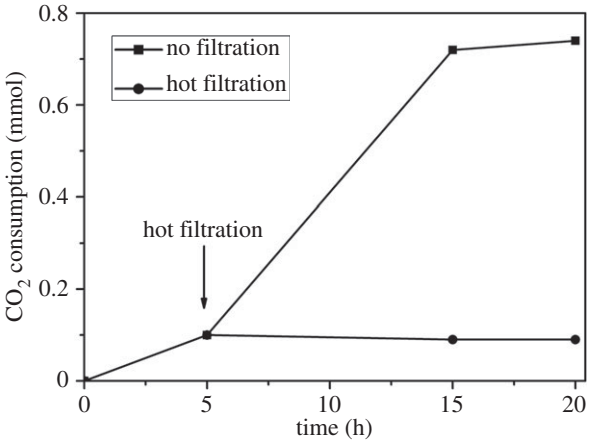

Figure 6. Hot filtration test for the Pt_1Ru_2/Fe_2O_3-catalysed CO_2 hydrogenation: (squares) typical reaction; (circles) the catalyst was filtered off. Reaction conditions were the same as those for entry 10 in table 2.

4. Conclusion

In summary, we have developed heterogeneous $PtRu/Fe_2O_3$ catalysts to produce C_{2+} alcohols from CO_2 hydrogenation in DMI. The bimetallic catalysts, especially the Pt_1Ru_2/Fe_2O_3, showed much higher catalytic activity and selectivity than the Pt/Fe_2O_3 or Ru/Fe_2O_3 catalysts for the reaction, indicating the excellent synergistic effect of the two metals in catalysing the reaction. The Pt_1Ru_2/Fe_2O_3 showed satisfactory activity and selectivity at relatively low temperature (e.g. 200°C). The reaction efficiency was improved significantly with increasing CO_2 pressure because the solubilities of both CO_2 and H_2 in the reaction mixture were enhanced. The catalyst could be re-used at least five times without reducing the activity and selectivity, indicating good stability of the catalyst. We believe that exploration of multi-metallic catalysts has a bright future for producing C_{2+} alcohols under milder conditions.

Authors' contributions. Z.H. and B.H. proposed the project, designed and conducted the experiments and wrote the manuscript; Q.Q., Z.Z., Q.M., H.Z. and Z.J. performed some experiments and discussed the work.

Downloaded from https://royalsocietypublishing.org/ on 04 March 2022

Competing interests. We have no competing interests.
Funding. The authors thank the National Natural Science Foundation of China (21373234, 21173239, 21321063) and the Chinese Academy of Sciences (KJCX2.YW.H30).

References

1. Federsel C, Jackstell R, Beller M. 2010 State-of-the-art catalysts for hydrogenation of carbon dioxide. *Angew. Chem. Int. Ed.* **49**, 6254–6257. (doi:10.1002/anie.201000533)
2. He M, Sun Y, Han B. 2013 Green carbon science: scientific basis for integrating carbon resource processing, utilization, and recycling. *Angew. Chem. Int. Ed.* **52**, 9620–9633. (doi:10.1002/anie.201209384)
3. Graciani J *et al.* 2014 Highly active copper-ceria and copper-ceria-titania catalysts for methanol synthesis from CO_2. *Science* **345**, 546–550. (doi:10.1126/science.1253057)
4. Studt F, Sharafutdinov I, Abild-Pedersen F, Elkjær CF, Hummelshøj JS, Dahl S, Chorkendorff I, Nørskov JK. 2014 Discovery of a Ni-Ga catalyst for carbon dioxide reduction to methanol. *Nat. Chem.* **6**, 320–324. (doi:10.1038/nchem.1873)
5. Rezayee NM, Huff CA, Sanford MS. 2015 Tandem amine and ruthenium-catalyzed hydrogenation of CO_2 to methanol. *J. Am. Chem. Soc.* **137**, 1028–1031. (doi:10.1021/ja511329m)
6. Choi Y, Liu P. 2009 Mechanism of ethanol synthesis from syngas on Rh (111). *J. Am. Chem. Soc.* **131**, 13 054–13 061. (doi:10.1021/ja903013x)
7. Prieto G *et al.* 2014 Design and synthesis of copper-cobalt catalysts for the selective conversion of synthesis gas to ethanol and higher alcohols. *Angew. Chem. Int. Ed.* **53**, 6397–6401. (doi:10.1002/anie.20142680)
8. Kusama H, Okabe K, Sayama K, Arakawa H. 1997 Ethanol synthesis by catalytic hydrogenation of CO_2 over Rh-Fe/SiO_2 catalysts. *Energy* **22**, 343–348. (doi:10.1016/S0360-5442(96)00095-3)
9. Kusama H, Okabe K, Sayama K, Arakawa H. 1996 CO_2 hydrogenation to ethanol over promoted Rh/SiO_2 catalysts. *Catal. Today* **28**, 261–266. (doi:10.1016/0920-5861(95)00246-4)
10. Kurakata H, Izumi Y, Aika K. 1996 Ethanol synthesis from carbon dioxide on TiO_2-supported [Rh_{10}Se] catalyst. *Chem. Commun.* **3**, 389–390. (doi:10.1039/CC9960000389)
11. Izumi Y, Kurakata H, Aika K. 1997 Ethanol synthesis from carbon dioxide on [Rh_{10}Se]/TiO_2 catalyst characterized by X-ray absorption fine structure spectroscopy. *J. Catal.* **175**, 236–244. (doi:10.1006/jcat.1998.1998)
12. Nieskens DLS, Ferrari D, Liu Y, Kolonko Jr R. 2011 The conversion of carbon dioxide and hydrogen into methanol and higher alcohols. *Catal. Commun.* **14**, 111–113. (doi:10.1016/j.catcom.2011.07.020)
13. Li S, Guo H, Luo C, Zhang H, Xiong L, Chen X, Ma L. 2013 Effect of iron promoter on structure and performance of K/Cu–Zn catalyst for higher alcohols synthesis from CO_2 hydrogenation. *Catal. Lett.* **143**, 345–355. (doi:10.1007/s10562-013-0977-7)
14. Inui T, Yamamoto T, Inoue M, Hara H, Takeguchi T, Kim JB. 1999 Highly effective synthesis of ethanol by CO_2-hydrogenation on well balanced multi-functional FT-type composite catalysts. *Appl. Catal. A* **186**, 395–406. (doi:10.1016/S0926-860X(99)00157-X)
15. Tominaga K, Sasaki Y, Saito M, Hagihara K, Watanabe T. 1994 Homogeneous Ru-Co bimetallic catalysis in CO_2 hydrogenation: the formation of ethanol. *J. Mol. Catal.* **89**, 51–56. (doi:10.1016/0304-5102(93)E0287-Q)
16. Arakawa H *et al.* 2001 Catalysis research of relevance to carbon management: progress, challenges, and opportunities. *Chem. Rev.* **101**, 953–996. (doi:10.1021/cr000018s)
17. Satthawong R, Koizumi N, Song C, Prasassarakich P. 2013 Bimetallic Fe-Co catalysts for CO_2 hydrogenation to higher hydrocarbons. *J. CO_2 Util.* **3–4**, 102–106. (doi:10.1016/j.jcou.2013.10.002)
18. Jiang X, Koizumi N, Guo X, Song C. 2015 Bimetallic Pt-Cu catalysts for selective CO_2 hydrogenation to methanol. *Appl. Catal. B* **170–171**, 173–185. (doi:10.1016/j.apcatb.2015.01.010)
19. Alayogl S, Nilekar AU, Mavrikakis M, Eichhorn B. 2008 Ru-Pt core-shell nanoparticles for preferential oxidation of carbon monoxide in hydrogen. *Nat. Mater.* **7**, 333–338. (doi:10.1038/nmat2156)

20. An N, Yu Q, Liu G, Li S, Jia M, Zhang W. 2011 Complete oxidation of formaldehyde at ambient temperature over supported Pt/Fe_2O_3 catalysts prepared by colloid-deposition method. *J. Hazard. Mater.* **186**, 1392–1397. (doi:10.1016/j.jhazmat.2010.12.018)
21. Liu M, Zhang J, Liu J, Yu WW. 2011 Synthesis of PVP-stabilized Pt/Ru colloidal nanoparticles by ethanol reduction and their catalytic properties for selective hydrogenation of ortho-chloronitrobenzene. *J. Catal.* **278**, 1–7. (doi:10.1016/j.jcat.2010.11.009)
22. Sunol JJ, Bonneau ME, Roue L, Guay D, Schulz R. 2000 XPS surface study of nanocrystalline Ti-Ru-Fe materials. *Appl. Surf. Sci.* **158**, 252–262. (doi:10.1016/S0169-4332(00)00019-2)
23. Chang FW, Roselin LS, Ou TC. 2007 Hydrogen production by partial oxidation of methanol over bimetallic Au-Ru/Fe_2O_3 catalysts. *Appl. Catal. A* **334**, 147–155. (doi:10.1016/j.apcata.2007.10.003)
24. Venugopal A, Aluha J, Mogano D, Scurrell MS. 2003 The gold-ruthenium-iron oxide catalytic system for the low temperature water-gas-shift reaction. The examination of gold-ruthenium interactions. *Appl. Catal. A* **245**, 149–158. (doi:10.1016/S0926-860X(02)00649-X)
25. Wu CT, Yu KMK, Liao F, Young N, Nellist P, Dent A, Kroner A, Tsang SCE. 2012 A non-syngas catalytic route to methanol production. *Nat. Commun.* **3**, 1050. (doi:10.1038/ncomms2053)
26. Paalanen P, Weckhuysen BM, Sankar M. 2013 Progress in controlling the size, composition and nanostructure of supported gold-palladium nanoparticles for catalytic applications. *Catal. Sci. Technol.* **3**, 2869–2880. (doi:10.1039/C3CY00341H)
27. Luo W, Sankar M, Beale AM, He Q, Kiely CJ, Bruijnincx PCA, Weckhuysen BM. 2015 High performing and stable supported nano-alloys for the catalytic hydrogenation of levulinic acid to γ-valerolactone. *Nat. Commun.* **6**, 6540. (doi:10.1038/ncomms7540)
28. Zhao F, Fujita S, Akihara S, Arai M. 2005 Hydrogenation of benzaldehyde and cinnamaldehyde in compressed CO_2 medium with a Pt/C catalyst: a study on molecular interactions and pressure effects. *J. Phys. Chem. A.* **109**, 4419–4424. (doi:10.1021/jp050049x)
29. Peng L, Zhang J, Xue Z, Han B, Sang X, Liu C, Yang G. 2014 Highly mesoporous metal-organic framework assembled in a switchable solvent. *Nat. Commun.* **5**, 5465. (doi:10.1038/ncomms5465)
30. Akien GR, Poliakoff M. 2009 A critical look at reactions in class I and II gas-expanded liquids using CO_2 and other gases. *Green Chem.* **11**, 1083–1100. (doi:10.1039/B904097H)

Downloaded from https://royalsocietypublishing.org/ on 04 March 2022